

Proceedings of the Institution of Mechanical Engineers, Part E: Journal of Process Mechanical Engineering

<http://pie.sagepub.com/>

Prediction of two-phase flow through a safety relief valve

Wael Elmayyah and William Dempster

Proceedings of the Institution of Mechanical Engineers, Part E: Journal of Process Mechanical Engineering published online 15 August 2012

DOI: 10.1177/0954408912453407

The online version of this article can be found at:

<http://pie.sagepub.com/content/early/2012/07/23/0954408912453407>

Published by:



<http://www.sagepublications.com>

On behalf of:



[Institution of Mechanical Engineers](http://www.institutionofmechanicalengineers.org)

Additional services and information for *Proceedings of the Institution of Mechanical Engineers, Part E: Journal of Process Mechanical Engineering* can be found at:

Email Alerts: <http://pie.sagepub.com/cgi/alerts>

Subscriptions: <http://pie.sagepub.com/subscriptions>

Reprints: <http://www.sagepub.com/journalsReprints.nav>

Permissions: <http://www.sagepub.com/journalsPermissions.nav>

>> [OnlineFirst Version of Record](#) - Aug 15, 2012

[What is This?](#)

Prediction of two-phase flow through a safety relief valve

Wael Elmayyah¹ and William Dempster²

Proc IMechE Part E:
J Process Mechanical Engineering
0(0) 1–14
© IMechE 2012
Reprints and permissions:
sagepub.co.uk/journalsPermissions.nav
DOI: 10.1177/0954408912453407
uk.sagepub.com/jpme



Abstract

Safety relief valves are necessary elements in any pressurised system. The flow inside the safety relief valve shows a number of interesting, yet complicated, features especially when a two-phase flow is involved. Consequently, developing an efficient and accurate means for predicting the safety relief valve performance and understanding the flow physics is a demanding objective. In this article, the ability of a two-phase mixture model to predict the critical flows of air and water through a safety valve is examined. An industrial refrigeration safety relief valve of $\frac{1}{4}$ " inlet bore size has been tested experimentally over a pressure range of 6–15 barg and air mass qualities from 0.23 to 1 when discharging to near atmospheric conditions for a range of valve lift positions. A two-dimensional mixture model consisting of mixture mass, momentum and energy equations, combined with a liquid mass equation and the standard k- ϵ turbulence model for mixture turbulent transport has been used to predict the two-phase flows through the valve. The mixture model results have been compared with the homogenous equilibrium model and the homogenous non-equilibrium model adopted by the ISO standard. It has been shown that the mixture model can be used satisfactorily to predict the mass flows for the above conditions. Overall, the accuracy of the two-phase air mass flow for given inlet liquid flow rates can be predicted to within 15%.

Keywords

Two-phase flow, critical mass flow, mixture model, computational fluid dynamics, safety relief valve

Date received: 25 November 2011; accepted: 11 June 2012

Introduction

A safety relief valve (SRV) is one of the most important safety devices in any safety system. This valve is designed and used to protect a pressurised system against excessive operating pressure. They are required to open at a predetermined system pressure and to discharge an amount of fluid to ensure a pressure reduction and then to close after the normal system pressure has been restored. Many industries including automotive, printing, aerospace and power plants use SRVs. The gas flow behaviour through SRVs is highly compressible and is characterised by viscous effects, turbulence, flow separation, critical flow conditions and shock waves. These effects limit the exit mass flow and may affect adversely on the system resulting in noise and vibration. Additional complexity arises when two-phase flow occurs in SRVs. Two-phase flow can be accompanied by mass, momentum and heat exchange between phases, which makes it more difficult

to predict the flow behaviour since these processes are less well understood. However, it is well known that two-phase flow imposes more limiting conditions due to compressibility, small geometries and high speed flow conditions since critical flow arise much more easily and imposes more limiting discharge flow rates. One of the most commonly used SRVs is the conventional spring loaded SRV. It is cheap, easy to install, maintain and use. In this study a conventional spring loaded SRV commonly found in the refrigeration industry has been used to investigate the physical and modelling issues that can occur in relief valves.

¹Military Technical College, Egyptian Armed Forces, Cairo, Egypt

²Department of Mechanical Engineering, University of Strathclyde, UK

Corresponding author:

Wael Elmayyah, Military Technical College, Egyptian Armed Forces, Cairo, Egypt.

Email: elmayyah@yahoo.co.uk

Figure 1 shows a cross section of the assembled valve and has a $\frac{1}{4}$ " inlet diameter to provide dimensional reference. The valve consists primarily of a moveable piston that is loaded by a spring to the required relief pressure. The spring is retained by a gland that can be adjusted to the required relief pressure. The piston has a sealing face which with sufficient spring load will contain the pressure of the system. When the system pressure exceeds the set pressure the piston will lift off the valve seat and allow mass to discharge through the available flow area. Increasing system pressure results in an increased lift and greater discharge flows until the piston movement reaches a limit stop or the limits in the compressibility of the spring. This straight through flow design geometry can be more of a challenge to model and design compared with the more common right-angled flow design due to the compact nature of the construction resulting in high levels of internal pressure and multiple choke points. However, manufacturing costs tend to be lower. In this study the objectives were to investigate the ability of a mixture model of the multiphase air water flow to predict the critical flow conditions in the safety valve. Steady flow conditions through the valve are examined both experimentally and computationally and are assumed to represent the valve flows when quasi-static conditions prevail. The two-phase flow conditions are generally high-speed flows and dominated by the annular or dispersed flow regimes. The mixture model is a simplified model of the full multiphase model and is considered a good alternative when simulating a dilute flow of droplets of liquid in a gas. In this work the commercial code Fluent 6.3.2 has been used as a vehicle to examine this model. The purpose of the study is also to compare simplified but generally used models for critical flow predictions such as the homogenous equilibrium model (HEM) and the homogenous non-

equilibrium model (HNE) so that the model difference can be assessed and quantified.

Background

A number of simplified models (algebraic based) exist to calculate the two-phase mass flow rates through SRVs and have been adopted by the international standards such as ISO, ASME and API for sizing purposes. The two-phase flow models are based on either the HEM or the HNE models. In general, these models consider the SRV as an ideal convergent-divergent nozzle and an empirically determined discharge coefficient is applied according to the model used. A special case of the HEM is called the ω method. The ω is named from the ω parameter which was first introduced by Leung¹ in 1986 and then modified in 1995 by the same author. The ω parameter is a compressibility factor defining an equation of state for the two-phase flow. The ω models are easy to use and depend only on the stagnation condition but still need the single-phase discharge coefficient of the gas and liquid supplied by the manufacturer or obtained experimentally. Diener and Schmidt² improved the ω method to extend its limits at lower qualities. This model called the homogeneous non-equilibrium model-Diener-Schmidt (HNE-DS) was improved by introducing a boiling delay coefficient, N , based on the mass quality at the critical cross section to account for the thermal non-equilibrium. Another modification was added by the same authors to account for the mechanical non-equilibrium due to friction between phases by introducing a correlation for the slip velocity. The adoption of these models by international standard organisations have established them as the most proven of the available methods. For example the ISO 4126-10³ adopted the HNE-DS model with a mechanical equilibrium assumption only while API 520 recommends an ω model. The predictive capability of these models has been discussed by Schmidt and Egan⁴ and Moncalvo and Friedel⁵ who showed that the ISO 4126-10 approach is the most accurate model to size SRVs under two-phase flow, although it oversized the valves at all working conditions. The ISO calculation approach is commonly used to calculate the critical mass flow rate for the fully open valve conditions occurring at maximum lift and do not provide for the valve flow-lift characteristics, which are essential in determining the opening and closing behaviour of a valve. However, in principle, given the correct discharge coefficients they have the ability to calculate the discharge flow rate at different lifts. Since detailed measurements of the internal flow conditions of SRVs tend to be prohibitive for both single-phase and two-phase flows due to access, geometry size, pressure

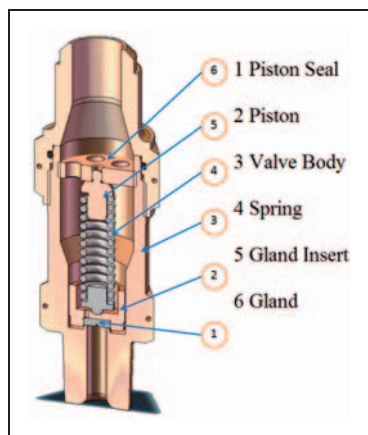


Figure 1. Safety relief valve assembly.

conditions and flow complexity the attempt to use computational fluid dynamics (CFD)-based modelling to provide both global and local flow details has been sought. Although CFD has been used successfully to predict the flow in SRVs under single-phase flow conditions by Dempster et al.⁶ and Dempster and Elmayyah⁷ there is a scarcity of studies for predicting two-phase flow through SRVs. However, some of the published two-phase computational studies suggest that it may be possible to use CFD for SRVs analysis. In this respect, the convergent divergent nozzle can be considered the nearest geometry to the SRV. Pougatch⁸ developed a two-fluid model to predict a high volume fraction water–air flow in a convergent divergent nozzle. The two-fluid Eulerian–Eulerian model with the standard k-e turbulence model showed good agreement with the experimental results. This simple geometry problem with two component frozen two-phase flow has provided a basic understanding of using CFD for predicting two-phase flow. Brennan⁹ used the mixture model to investigate a solid–liquid air flow at a separator cyclone. The Reynolds Stress turbulent model was used to account for the swirl and flow reversal that dominate the flow through the cyclone separator. The model prediction for the density profiles showed qualitatively correct results, whereas the predicted segregation was larger compared with the measured one by the gamma ray tomography. The most extensive study of two-phase modelling of high speed two-phase flows and representative of the flows in relief valves is discussed in the monograph by Staedtke,¹⁰ which suggest that a mixture modelling approach may be adequate. To date and to the authors' knowledge no published modelling studies on two-phase flow through SRVs have been found in the literature. The work presented here therefore examines the application of an established two-phase mixture modelling approach and assess' its capability against

the standard ISO calculation methods and validates all of these models against experimentally determined values of mass flow rate for various liquid mass fraction and upstream pressure conditions.

Experimental setup and procedures

The purpose of the experimental work is to obtain the liquid and air flow rates that the valve can discharge under controlled upstream pressure conditions. This can be done at various valve piston lift positions, which corresponds to different valve flow areas and allows flow-lift characteristics to be produced. The upstream air pressure is maintained constant during each test for variations in different water flow rates injected into the valve. Thus for each test condition, determined by the control of the piston lift, upstream pressure and liquid flow rate, the air mass flow becomes the uncontrolled quantity determined by the circumstances of the two-phase interaction with the valve. The water is injected into the flowing air upstream of the valve allowing them to mix prior to entering the valve. A converging nozzle has been used to facilitate the injection and mixing of the fluid. Downstream of the valve, a separator with the necessary connections and adaptors is used to separate the water and the air. The water collected in the separator also acts as a water supply for the water injection pump. The test rig, Figure 2, consists of a 100 mm (4 in.) diameter pipe (1) connected to a compressed air system to deliver high pressure (1–15 bar) compressed air to the valve. The tested safety valve (3) is connected to the pipe via a brass converging section (2) with inlet diameter 29 mm and outlet diameter 6.35 mm to adapt to the valve entrance. An injection nozzle (4) is fitted in the converging section to inject the water. The injection nozzle is a 4 mm tube with a closed end and an exit orifice positioned on the side wall facing downstream

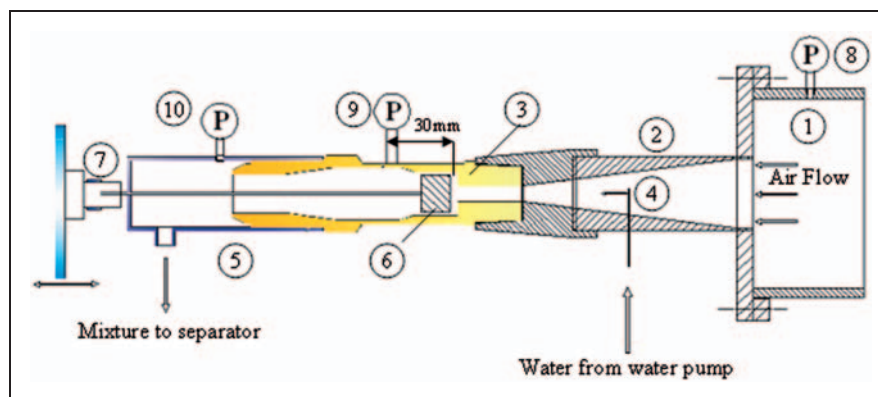


Figure 2. Test rig construction scheme.

and located at the centre of the tube. The orifice generates a well-distributed dispersed water flow. A PVC tube (5) with a 50 mm diameter side exit is connected to the valve to direct the mixture to the separator. This is maintained close to atmospheric pressure. The PVC piece was designed such that it has a minimum resistance to the exit flow. It has a pressure tapping fitted to the PVC piece to measure the pressure at the valve outlet (Figure 2). The valve piston (6) is attached to a 250 mm long 6 mm diameter rod which passes through the far end of the PVC tube end and is connected to a lead screw and traverse table (7) allowing the piston position to be adjusted. The piston movement is in the range of 0–5 mm and was measured by a Mitutoyo digital dial indicator with sensitivity of 0.001 mm. To allow the connecting rod to be inserted the original valve required to be modified by removing the spring and associated gland/spring inserts resulting in a modified gland being used. While these changes detracted from the correct representation of the relief valve, their effect on the mass flows have been found to be minimal from additional testing conducted with these components in place.

The water injection system consists of a positive displacement diaphragm water pump (Hydra Cell G20) connected to the injection nozzle (4) via a high pressure hose. The pump has a maximum flow rate of 3.5 L/min and will deliver the flow independently of the downstream pressure up to 100 bar. The pump is driven by an AC motor controlled by a speed controller, which allows fine adjustment for the water flow rate needed. Upstream of the injection nozzle, a flow meter (Platon GMT) is fitted to facilitate measurement of the water flow rate; it has a flow rate range of 0.4–4 L/min and has an accuracy of 2% of the range. A pressure relief valve is attached to the pump outlet to protect the circuit from any unexpected high pressure. A bladder accumulator (Flow Guard DS-20) is also connected to the pump outlet to damp the pulsating water flow rate from the pump. The air flow rate was measured using a Sierra Vortex mass flow meter (Innova mass 240) and

accurate to <1% of reading. The upstream pressure, back pressure and the outlet pressure are measured by three Bourdon pressure gauges as shown, Figure 2 (8, 9 and 10, respectively). Table 1 shows the experimental test matrix, which has been carried out on the valve. These range of pressures and water flow rates give a working air flow rate from 0.015 to 0.86 kg/s and a water mass fraction range from 0 to 0.71.

Mathematical models

The mixture model

The mixture model is used in this study to predict the two-phase flow conditions in the safety valve. The mixture model is a simplified model of the full Eulerian–Eulerian multiphase model. This model is considered a good alternative in simulating dilute flows of droplets of liquid in gas, suspensions of solid particles in a gas or small bubbles in a liquid. In the high-speed dispersed flows studied here the gas and liquid velocities may at times be considerably different due to the short acceleration paths in the valve. Also while no phase change is expected, the dominant gas flow will reduce in temperature as the gas expands and lead to thermal non-equilibrium effects arising since the liquid thermal inertia is significantly higher preventing temperature changes at the same rate as the gas. In the mixture model used here only the effects of velocity slip are accounted for. The thermal non-equilibrium is not and may result in a divergence from reality as the liquid flow rate is increased. The mixture model equations are fully described by Manninen¹¹ and in the Fluent Technical Manuals.¹² For comparison purposes, the HEM developed by Darby¹³ and The HNE-DS developed by Diener and Schmidt² have been used here. The HNE-DS model accounts for thermal non-equilibrium and slip between phases. The ISO standard ISO-4162-10 adopted the HNE-DS model for selecting SRVs for two-phase flow, but with no slip defined between the phases.

Computational model

A two-dimensional axisymmetric model has been shown to provide adequate prediction for the mass flow rate for single-phase air flow in a similar valve geometry.^{6,7} The two-dimensional axisymmetric model is much more computationally efficient than the three-dimensional model. A two-dimensional axisymmetric model has been developed to represent the safety valve geometry and the converging section, which includes the injection nozzle. The flow areas between the piston and the valve body and the gland flow areas are strictly three-dimensional geometries. However, modelling these as two-dimensional

Table 1. Experimental test matrix for two-phase flow.

Water flow rate (kg/s)	Test pressure (barg)			
	6.9	8.6	10.3	12.07
0.00	✓	✓	✓	✓
0.01			✓	✓
0.02		✓	✓	✓
0.03	✓	✓	✓	✓
0.04	✓	✓	✓	✓
0.05	✓	✓	✓	✓

equivalent annulus areas, as shown in Figure 3, has been found adequate as indicated in the single-phase studies of Dempster et al.⁶ The computational mesh has a total of 11,350 quadrilateral cells distributed giving an average mesh density of 8 cells/mm². A more dense mesh of 20,000 quadrilateral cells has been used to examine the grid independency; there was no significant improvement to the solution of the discharge flow rate. The difference in air flow rate was 0.00001 kg/s so the cell number was kept about 14,000 in all cases. The injection nozzle has been introduced as a water inlet with the same orifice diameter. The boundary conditions used are the pressure inlet, pressure outlet, mass flow inlet and stationary walls.

Boundary conditions and solution

The boundary conditions are applied at the converging section inlet, valve outlet, injecting nozzle inlet and the valve and the converging section walls. Walls of the valve and the converging section were defined as stationary walls. At the inlet boundary, which is an air only inlet, the stagnation pressure, static pressure and stagnation temperature are applied; in addition an initial value for the turbulence intensity and the hydraulic diameter are introduced. At the outlet boundary the static pressure and the stagnation temperature are applied. At the injecting nozzle, which is a water

only inlet, the stagnation pressure, stagnation temperature and the water mass flow rate is defined; in addition an initial value for the turbulence intensity and the hydraulic diameter are introduced.

The discretisation scheme used for the continuity, momentum, energy, turbulent kinetic and turbulent dissipation energy equations was second-order upwind for the convection terms and second-order central difference for the diffusion terms. For the volume fraction equation the discretisation scheme was first-order upwind for the convection terms and second-order central difference for the diffusion terms. The convergence criterion was based on the residual values of the calculated variables, i.e. mass continuity, velocity components, energy, turbulent kinetic energy and turbulent dissipation energy. The threshold values were 1×10^{-3} for all variables except for the energy which was 1×10^{-6} and for the mass continuity, 1×10^{-4} . All cases have converged in about 60 min on a 2.4 GHz desktop PC. The pressure range used was 7–14 barg (100–200 psig) to allow model validation by the experimental results.

Results and discussion

Experimental results

The variation in mass flow with piston lift is used to provide a complete description of the valve discharge

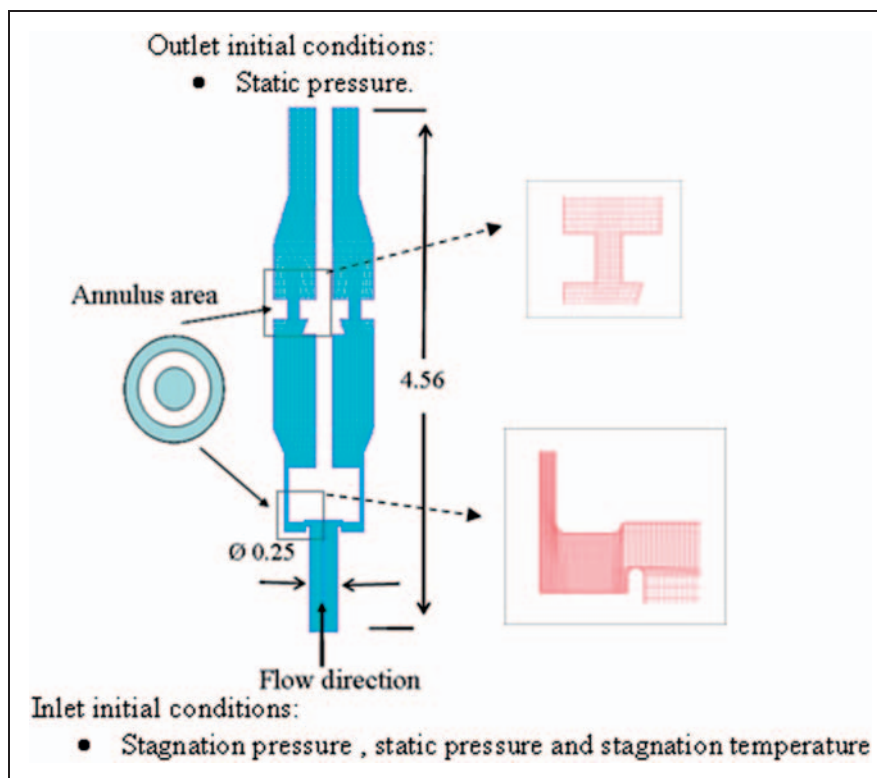


Figure 3. Computational grid of the valve (diameter in inches).

characteristics with respect to the piston movement. Figures 4 and 5 show the measured air mass flow rates and mixture mass flow rates at an inlet pressure of 12.07 barg (175 psi) at different water flow rates (0–0.05 kg/s). These results indicate the critical flow conditions at each piston lift location and cover a gas mass fraction range of 0.23–1. These figures indicate that the mass flow increases rapidly with lift and then reaches an approximately constant mass flow for each

injected liquid flow rate becoming independent of piston lift. Figure 4 shows that the air flow rate decreases with an increase in the water flow rate, while the total mixture flow rate is increased (Figure 5). This behaviour indicates that the air flow rate is decreased by an amount less than the water flow rate is increased. Figure 4 shows that the air flow-lift characteristics in the two-phase flow follow the air flow-lift behaviour for the single-phase tests. This suggests

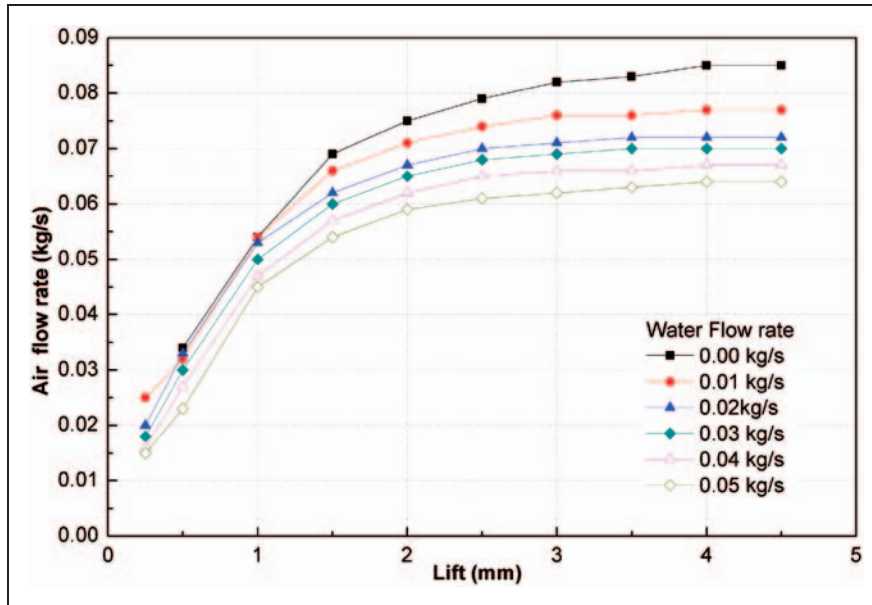


Figure 4. Air flow-lift at 12.07 barg (175 psi).

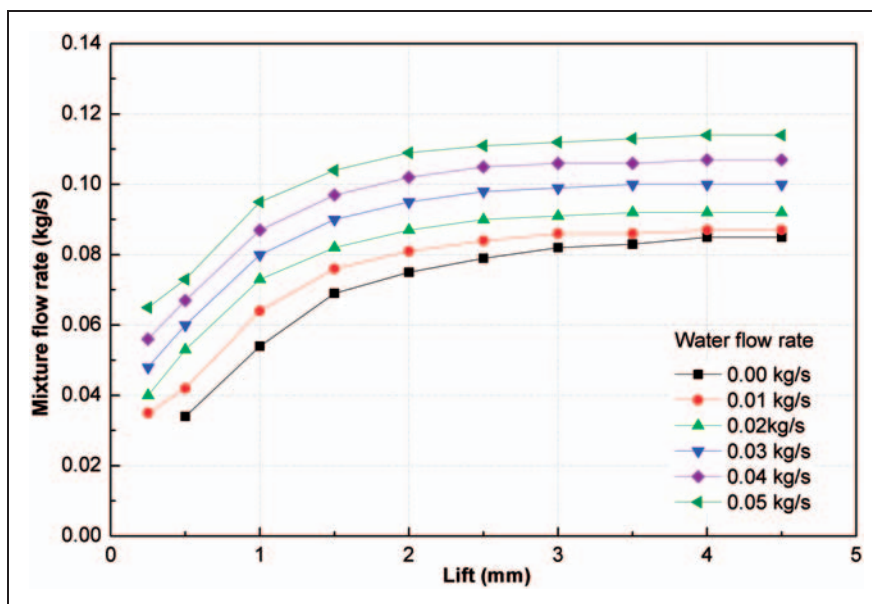


Figure 5. Mixture flow-lift at 12.07 barg (175 psi).

that the choking planes for the mixture flow are similar to single-phase tests,⁷ which will be shown later. It is apparent from Figure 4 that with more water flowing through the valve, the less air flows and is a consequence of the critical flow requirements for the increased liquid flow.

CFD results

The application of the mixture model can provide considerable insight into the details and flow structure

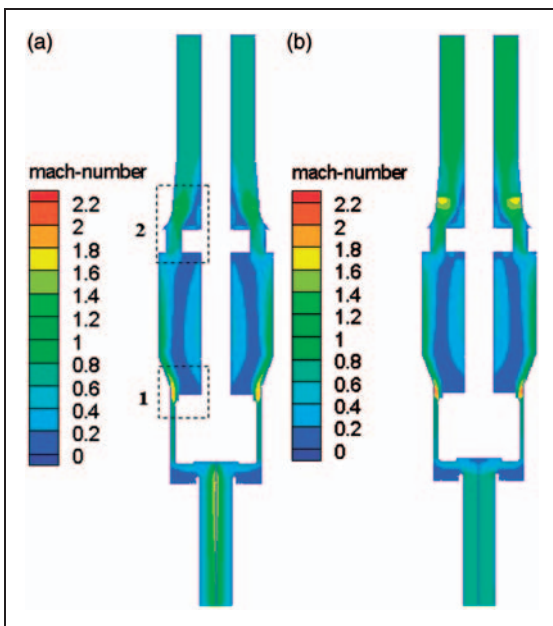


Figure 6. Contours of Mach number at single-phase air and 0.05 kg/s water flow rate, 3 mm lift and 12.07 barg: (a) mixture Mach number, (b) single-phase air Mach number.

within the valve. To illustrate this, the Mach number contours, slip contours and the water volume fraction contours are presented for a high piston lift position where the valve has reached its fully open condition and the mass flow has approximately reached its maximum value. The Mach number contours (Figure 6) can show the critical planes and how this affects the flow rate. From the slip contours (Figure 7), it can be shown whether the homogeneous flow assumption is valid or not. The water volume fraction at the critical planes significantly affects the flow rate as discussed before; this can be shown from the water volume fraction contours. Figure 6 presents the air and the mixture Mach number contours at 12.07 barg, 3 mm lift and 0.05 kg/s water flow rate. The definition shown in equation (1) based on homogeneous assumptions has been used. The Mach number for the mixture is defined as follows

$$M = U_m/a_{sm} \quad (1)$$

where U_m is the mixture velocity, and a_{sm} is the sonic speed in the mixture, which is defined for a homogeneous flow with air volume fractions higher than 0.9 as follows

$$a_{sm} = [(\gamma P)/(\alpha \rho_m)]^{0.5} \quad (2)$$

In Figure 6, it can be seen that the critical plane position is similar for both single-phase and two-phase conditions, which indicates similar flow-lift characteristics. The figures show that the flow accelerates at the valve entrance until the flow is choked at the exit of the annular channel between the piston and the valve body ($M=1$). A further expansion downstream of the choking plane results in supersonic conditions for a short

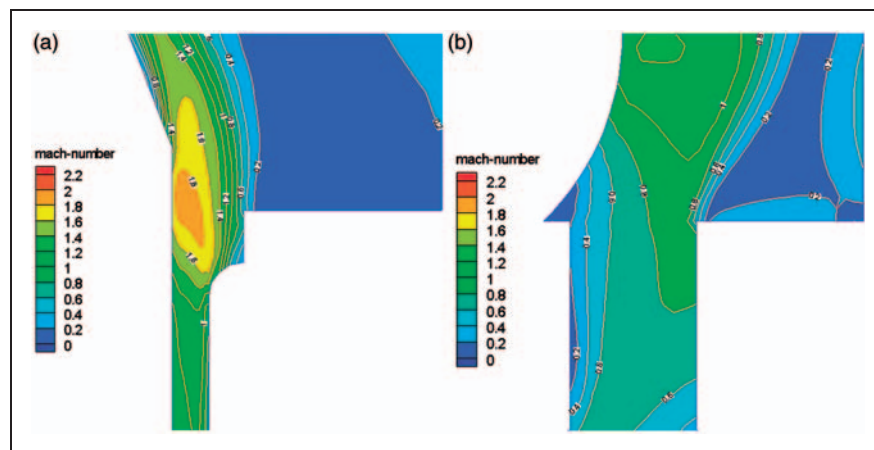


Figure 7. Contours of Mach number at 0.05 kg/s water flow rate, 3 mm lift and 12.07 barg at Area 1 and 2 (shown in Figure 6): (a) Area 1, (b) Area 2.

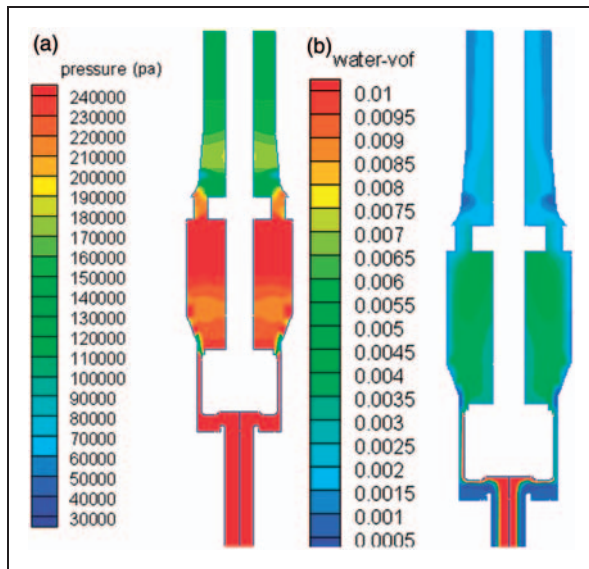


Figure 8. Contours of (a) static pressure and (b) water volume fraction at 4 mm lift and 12.07 barg.

distance before undergoing compression due to the gland geometry. The static pressure contours are shown in Figure 8(a). The flow behaviour is similar to the single-phase flow in terms of undergoing compression, expansion and the choking plane locations because of the high air volume fraction. Therefore the air Mach number contours is similar to the mixture contours but with different values due to the density difference between the air and the air–water mixture. The air Mach number reaches 1.4, while the mixture Mach number reaches 2. Upstream of the gland, the flow accelerates through the reduced gland area; however, the flow velocity remains subsonic. Figure 8 shows the water volume fraction and static pressure contours at a 4 mm lift with no gland and 0.05 kg/s water flow rate. From the figure it is shown that the water distribution is characterised by a core-based dispersed flow at the valve entrance centre axis then a dispersed flow around the piston but with a higher concentration of water droplets near the piston wall. The water volume fraction ranges from 0 to 0.01. Figure 9 presents the slip contours at 3 mm lift, 12.07 barg, and 0.01 and 0.05 kg/s water flow rate. The figure shows that the slip value is near zero at most of the flow regions. Only at the valve entrance at 0.01 kg/s water flow rate there is a slip value of 200 m/s. At 0.01 kg/s water flow rate, the water flow has a low velocity (6.4 m/s at the injection orifice). Therefore, the high air flow rate results in high slip values between the high velocity air and the low velocity water. However, the slip occurring at 0.01 kg/s has no significant effect on the air flow rate. Figure 10 presents the predicted flow–lift 0.01 kg/s with and without slip. It shows that accounting for the slip

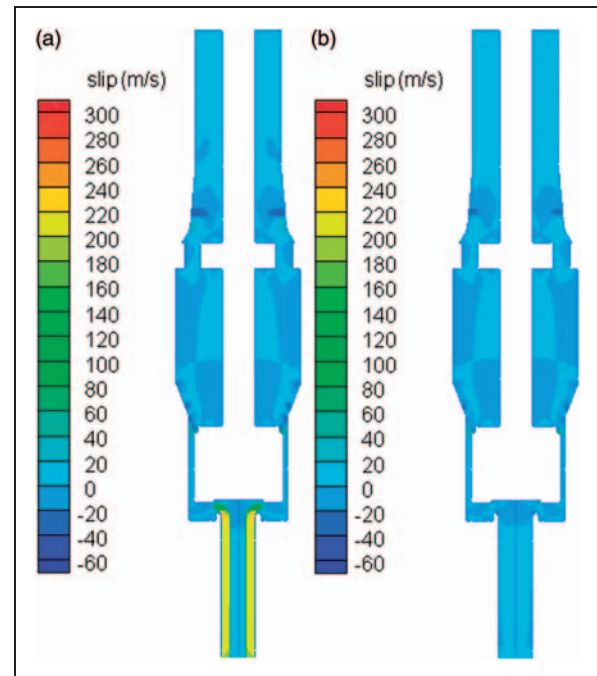


Figure 9. Contours of slip at 3 mm lift and 12.07 barg at (a) 0.01 and (b) 0.05 kg/s (with gland).

does not make any significant change for the flow rate. It can be concluded that as far as the mixture model is concerned a homogeneous assumption can be applied here. Therefore, the flow is considered a homogeneous flow and all cases presented were calculated without the slip equation. Since the slip will equal zero so the relative Reynolds number and the drag coefficient equal zero. Fluent provides the facility of disabling the drag and slip equations for a homogeneous flow assumption.

The water volume fraction at the critical plane will significantly affect the air flow rate as discussed before. Water volume fraction contours at the critical plane will give a better clarification. Figure 11 shows the water volume fraction at the critical plane at 3 mm lift and inlet pressure 12.07 barg. It is noticeable that at 0.05 kg/s water flow rate, the water droplets decrease the effective area available for the air to flow freely.

Simplified models predictions

Predictions of the discharge mass flow rate using the mixture model, the ISO (HNE-DS) method and the HEM method have been made for an upstream stagnation pressure of 8.6 barg and for the valve maximum lift of 5 mm, which corresponds to the maximum fully open flow area. Calculations have been carried out for the range of liquid flow rates investigated and compared with the experimental test data. The HNE-DS and the HEM methods are based on the liquid and gas discharge coefficient. The gas discharge coefficient

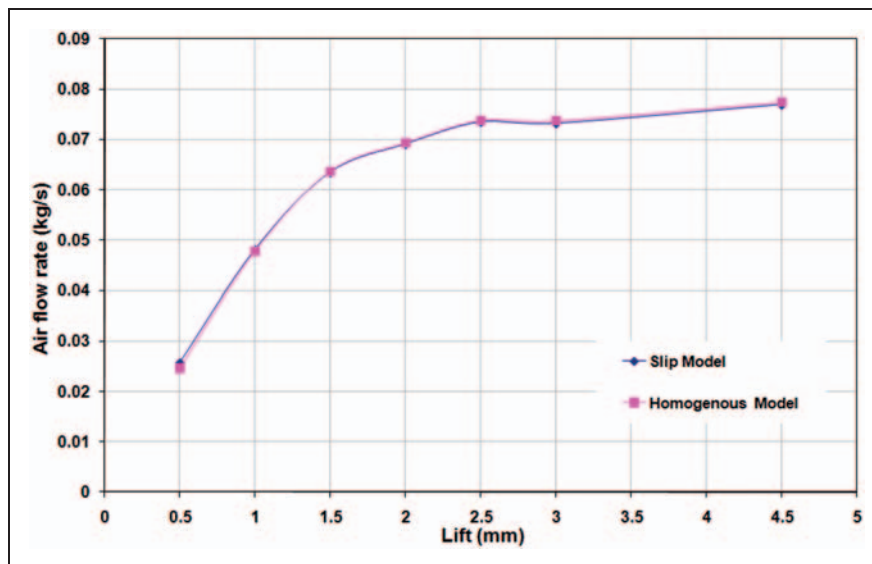


Figure 10. Predicted flow-lift characteristics of the slip and homogeneous models at 0.01 kg/s water flow rate and 12.07 barg pressure.

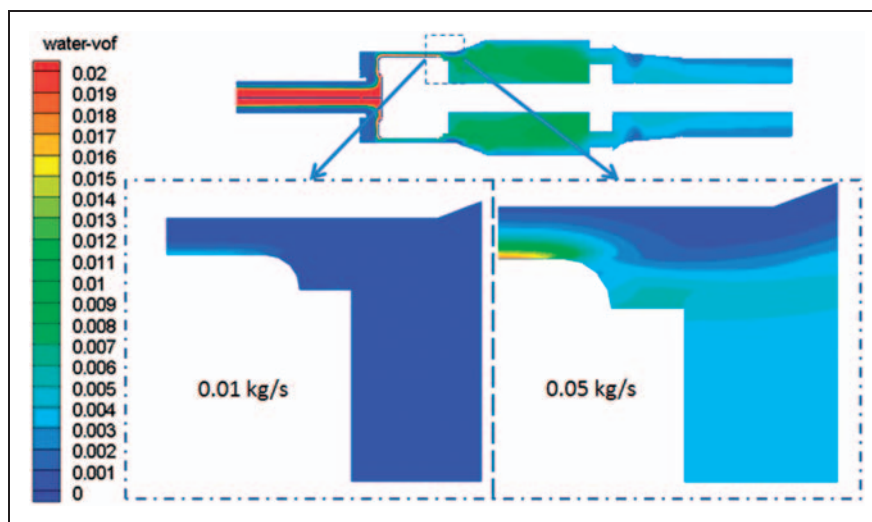


Figure 11. Water volume fraction at lift 3 mm and 12.07 barg.

has been determined experimentally at maximum lift and was found to be 0.89. The liquid discharge coefficient was not available experimentally and was found using CFD to be 0.5. However, the mixture flow rate was not sensitive to the liquid discharge coefficient due to the high air volume fraction. The comparison shows that the ISO model and the HEM reasonably predict the two-phase mass flow for this range of operating conditions. The ISO model accounts for the heat transfer between phases and gives a closer prediction of the discharge flow rates than the HEM. Unlike the simplified models, the CFD mixture model is based on the full geometry of the valve and accounts for the liquid

distribution effects. Thus, the CFD mixture model results are the closest to the experimental results and they follow the experimental results trend line. Figure 12 shows the prediction of the mixture mass flow rate by the ISO model, HEM and the CFD mixture model at 8.6 barg.

Results analysis

Figures 13 and 14 present a comparison of the CFD-based mixture model for the air mass flow rates or the mixture mass flow rates respectively for a 12.07 barg pressure and water flow rates of between 0.01 kg/s

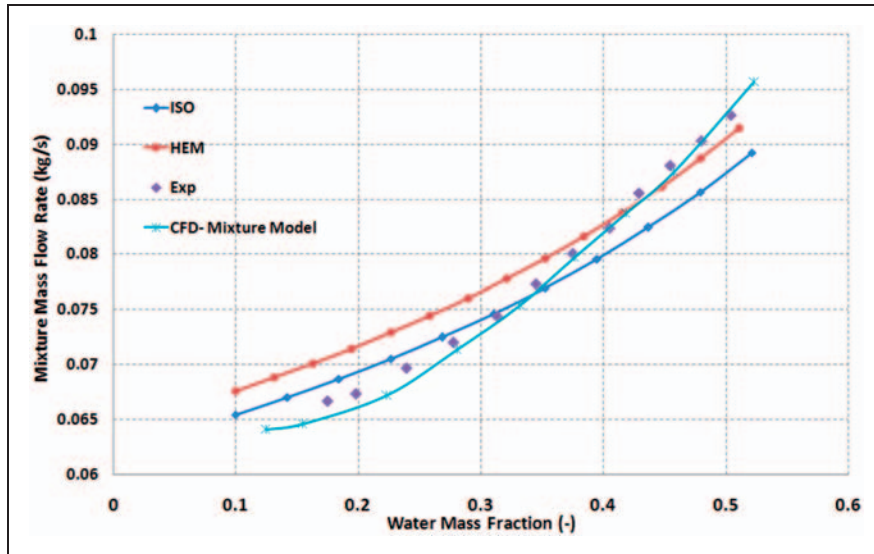


Figure 12. Mixture flow rate prediction by the ISO model, HEM and CFD mixture model at 8.6 barg at maximum lift (5 mm). HEM: homogenous equilibrium model; CFD: continuum fluid dynamics.

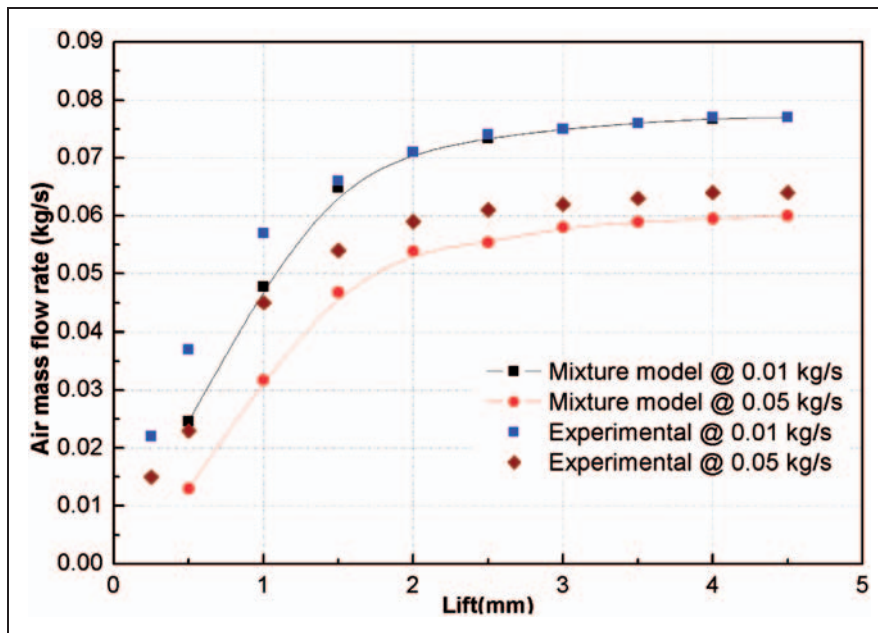


Figure 13. Air flow rate lift at 12.07 barg (175 psi).

and 0.05 kg/s against the experimental results. The figures show in general a good agreement between the predicted and experimental results at high lifts (1.5–4.5 mm), while less agreement is noticed at low lifts (0.25–1 mm). The figures also show that the mixture model prediction is more close to the experimental results at 0.01 kg/s water flow rate. The mixture model prediction shows reasonable agreement with the experimental results at higher lifts with low liquid mass

fraction (Figure 15). Also shown is that the accuracy of predicting the flow is less when the water flow mass fraction increases. Figure 15 presents the effect of the water mass fraction on the mixture model prediction accuracy. For example, at a stagnation pressure of 10.3 barg (150 psi), the deviation is 2.6% at water mass fraction 0.13 and it is 5.36% at 0.5.

On the other hand, at lower lifts the deviation of the predicted and the experimental results is larger; this is

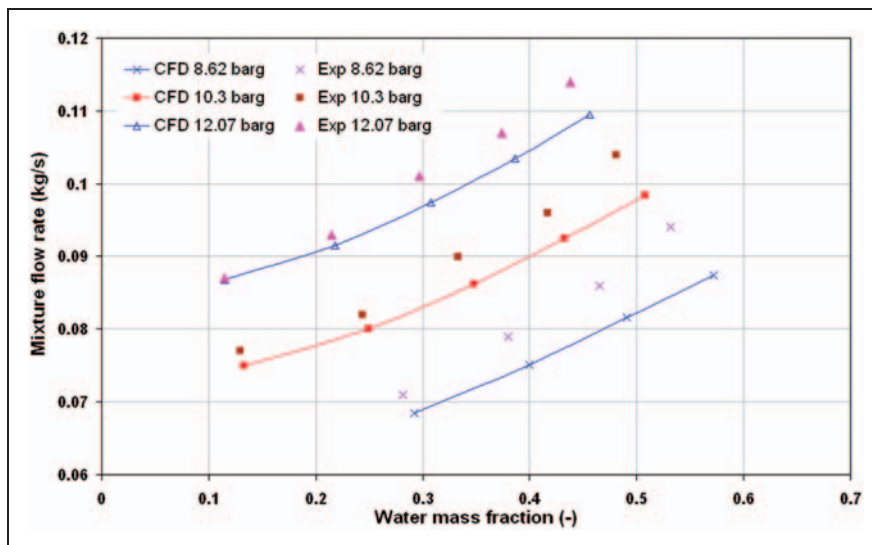


Figure 14. Mixture flow rate lift at 12.07 barg (175 psi).

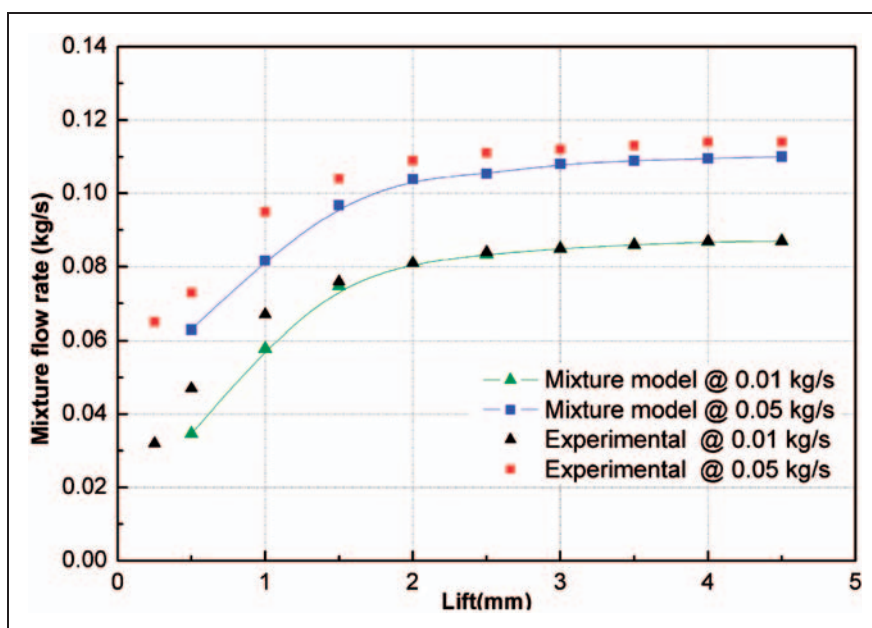


Figure 15. Effect of the water mass fraction on mixture flow rate at 4 mm lift and 12.07 barg.

shown in Figure 16. The figure shows the mixture flow rate at different water flow qualities. Figure 17 presents the percentage deviation of the predicted mixture flow rate with respect to the experimental results at 1 mm and 4 mm lift and shows better accuracy at lower water mass fraction. However, the accuracy is less at 1 mm lift at the same water mass fraction. Figure 18 shows the overall deviation of the predicted air mass flows results from the experimental results at 12.07 barg for all lifts and liquid mass flows and shows the typical errors expected of the mixture model. Around 88% of

the results fall within a 25% error band with the remaining data in the 25–40% deviation range occurring at low lifts. This difference in the mixture model accuracy of predicting the flow rate from low to high lifts may be due to a number of factors including the effects of inlet flow regime and the prediction of phase distributions and the accuracy of the valve seat geometric representation compared to the actual tested valve. For low lifts the choking point is located at the valve seat, which is at a different location compared to high lift conditions since the minimum area location changes

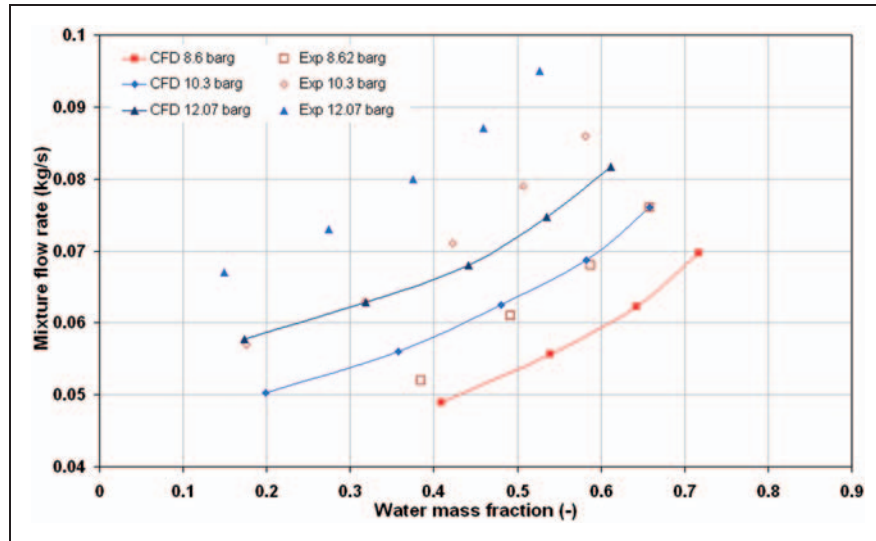


Figure 16. Effect of the water mass fraction on mixture flow rate at 1 mm lift.

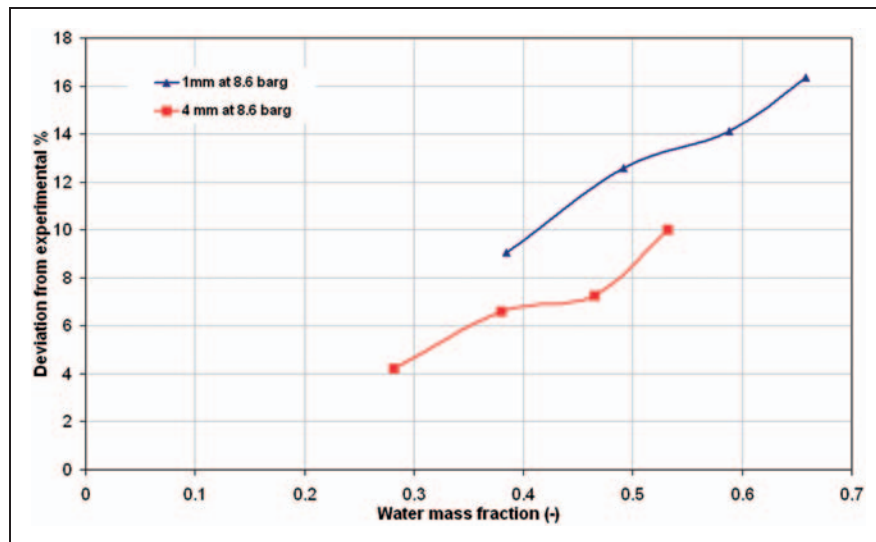


Figure 17. Deviation percent of the CFD results from the experimental results at 8.6 barg at 1 mm and 4 mm lift. CFD: continuum fluid dynamics.

as the lift increases. Thus modelling accuracy is dependent on how well the computational model represents the actual geometry and will be sensitive to the machining tolerances of the valve at these small lift conditions. Furthermore since the valve seat area is directly upstream of the injection point the effect of liquid distributions are likely to have more influence here. This combined with lower air flows imposes greater liquid mass fractions and the likely hood of non-equilibrium conditions imposes a greater challenge on the numerical prediction of the discharge flow rates at the lower lifts. Furthermore, there are indications that the Fluent mixture model shows a sensitivity to inlet flow

distributions greater than that indicated by the experimental data, particularly at the higher range of liquid mass qualities investigated here. A more in depth study is required to investigate this further.

Conclusions

An experimental approach has been developed for testing SRVs under two-phase flow. A test rig has been developed to facilitate the implementation and measurement of air water flow through SRVs for inlet pressure between 6 and 17 barg and inlet gas mass fractions between 0.3 and 1 (0 to 0.7 water mass fraction).

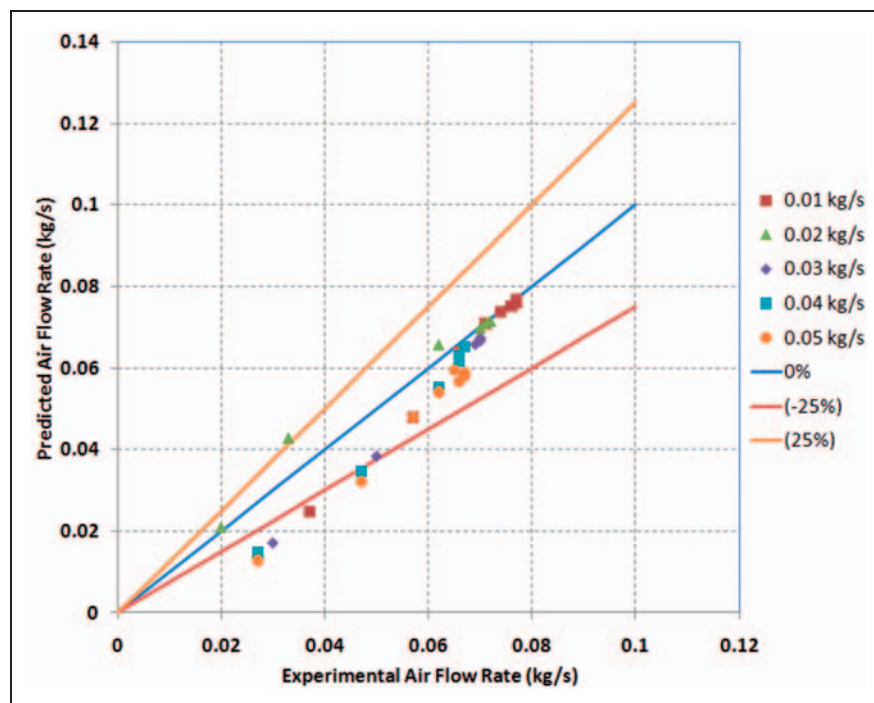


Figure 18. Deviation percent of the CFD results from the experimental results at 12.07 barg. CFD: continuum fluid dynamics.

The experimental approach, with the measurement of the air and water flow rate, pressures, temperature and lift, has been found satisfactory for obtaining the valve flow-lift and force lift characteristics at different test pressures and water mass fractions.

The experimentally measured flow-lift and force lift characteristics have helped in understanding the two-phase flow behaviour and quantified the accuracy of a two-phase mixture modelling approach for the prediction of discharge flow rates through a SRV. The following general points can be made regarding the results:

1. In general, the two-phase flow-lift characteristics have a similar behaviour to the single-phase flow characteristics.
2. At any fixed test pressure and lift, with a water flow increase the air flow decreases.
3. The CFD mixture model has shown the capability to give good details on the flow regime and flow properties distributions with identifying the critical planes.
4. Accounting for the slip does not have a significant effect on the flow prediction. Hence, the flow can be considered homogeneous.
5. The mixture model prediction for the mixture flow rate shows good agreement with the experimental results at high lifts with low water mass fraction. The deviation from the experimental results is only 0.5% at 0.11 water mass fraction. However, the accuracy of predicting the flow rate is less

when the water mass fraction increases. The deviation from the experimental results is 9% at 0.55 water mass fraction. At lower lifts the deviation of the predicted results from the experimental are larger and reach 16%.

6. The mixture model has shown to have a better agreement with the experimental results than the HEM, and the HNE-DS model adopted by ISO for predicting the mixture flow rate at fully open valve positions

Funding

This research was funded by the Egyptian Armed Forces and the University of Strathclyde.

References

1. Leung JC. A generalized correlation for one-component homogeneous equilibrium flashing choked flow. *AIChE Journal* 1986; 32(10): 1743–1746.
2. Diener R and Schmidt J. Extended omega-method applicable for low inlet mass flow qualities. Ludwigshafen, Germany, June 1998. 13th Mtg. ISO/TC185/WG1.
3. ISO 4126-10. *Safety devices for protection against excessive pressure – Part 10: Sizing of safety valves and connected inlet and outlet lines for gas/liquid two-phase flow*. Geneva: International Organization for standardization (ISO), 2004.
4. Schmidt J and Egan S. Case studies of sizing pressure relief valves for two-phase flow. *Chem Eng Technol* 2009; 32(2): 263–272.

5. Moncalvo D and Friedel L. Reproductive accuracy of safety valve two-phase mass flowcapacity models in case of air/water, resp., viscous liquid flow duty. *Forschung im Ingenieurwesen* 2005; 70(2): 133–138.
6. Dempster W, Lee CK and Deans J. Prediction of the flow and force characteristics of safety relief valves. In: *Proceedings of PVP2006-ICPVT-11 2006 ASME Pressure Vessels and Piping Division Conference*, Vancouver, Canada, July 2006.
7. Dempster W and Elmayyah W. A computational fluid dynamics evaluation of a pneumatic safety relief valve. In: *The 13th International Conference on Applied Mechanics and Mechanical Engineering (AMME)*, Cairo, Egypt, May 2008.
8. Pougatch K, Salcudean M, Chan E, et al. Modelling of compressible gas liquid flow in a convergent-divergent nozzle. *Chem Eng Sci* 2008; 63(16): 4176–4188.
9. Brennan MS. Multiphase CFD simulations of dense medium and classifying hydrocyclones. In: *Third International Conference on CFD in the Minerals and Process Industries CSIRO*, Melbourne, Australia, December 2003, pp.59–63.
10. Staedtke H. *Gas dynamic aspects of two-phase flow: hyperbolicity, wave propagation phenomena, and related numerical methods*. Weinheim: Wiley-VCH Verlag GmbH & Co. KGaA, 2006.
11. Manninen M, Taivassalo V and Kallio S. On the mixture model for multiphase flow. Technical Report, Technical Research Center of Finland, 1996.
12. Fluent 6.3 User Guide, 2006.
13. Darby R. On two-phase frozen and flashing flows in safety relief valves: recommended calculation method and the proper use of the discharge coefficient. *J Loss Prev Process Ind* 2004; 17(4): 255–259.

Appendix

Notation

M	Mach number
P	pressure (Pa)
U_m	mixture velocity component (m/s)
a_{sm}	sound speed in mixture (m/s)
α	air volume fraction
γ	heat capacity ratio
ρ_m	mixture density (kg/m^3)